

# Na<sup>+</sup> Channels at Postsynaptic Muscle Membrane Affects Synaptic Transmission at Neuromuscular Junction: A Simulation Study

Mufti Mahmud, *Member, IEEE*, M. Mostafizur Rahman, *Graduate Member, IEEE*, Stefano Vassanelli

**Abstract**—Motor movement is controlled by the brain through transmitting electrochemical signals to the muscle fibers that cause the contraction of the muscles. A motoneuron carrying the impulse creates a synapse with the muscle fiber which is known as Neuromuscular Junction (NMJ). The muscle infolds taking part in the synapse contains large amount of sodium channels. The current that passes through the narrow synaptic cleft affects the adjacent membranes electrical properties in turn modifies the synaptic transmission process. Considering this phenomenon we have studied the effect of sodium channels at the NMJ to find out its effect in the generation of extracellular potentials at the synaptic cleft of the junction. Through simulation results we confirm that the conductivity of the sodium channels present at the postsynaptic muscle membrane and the junction height affect the generation of the extracellular potentials at the junction which modifies the synaptic properties of the NMJ.

**Keywords**— Neuromuscular Junction; Synaptic Cleft; Sodium Channels; Channel Conductance; Action Potentials.

## I. INTRODUCTION

THE brain controls the motor movements by sending impulse mediated electrochemical signals which cause the muscle to contract. The motoneuron connects to the muscle fiber forming a synapse to ensure a rapid and efficient transmission of the impulse. This arriving impulse in the form of an action potential depolarizes the postsynaptic target muscle by transmitting excitation electrochemically and causing the muscle to contract. This special type of synapse is called the Neuromuscular Junction (NMJ). The mechanism of neurotransmitter conduction has studied extensively [1-6]. Due to the arriving impulse the voltage-dependent calcium channels at the presynaptic nerve terminal opens up increasing the Ca<sup>2+</sup> ions permeability which allows Ca<sup>2+</sup> ions

to flow in. This causes the vesicles to be fused with the endplate membrane and release neurotransmitter (Acetylcholine, ACh) at the synaptic cleft. The ACh diffuses at the cleft and binds with the Acetylcholine Receptors (AChR) resulting in opening of voltage-dependent sodium channels located at the postsynaptic muscle membrane. The inflow of sodium ions and outflow of potassium ions at the postsynaptic muscle membrane generate endplate synaptic potential (EPSP) and initiates an action potential [7] (fig. 1).

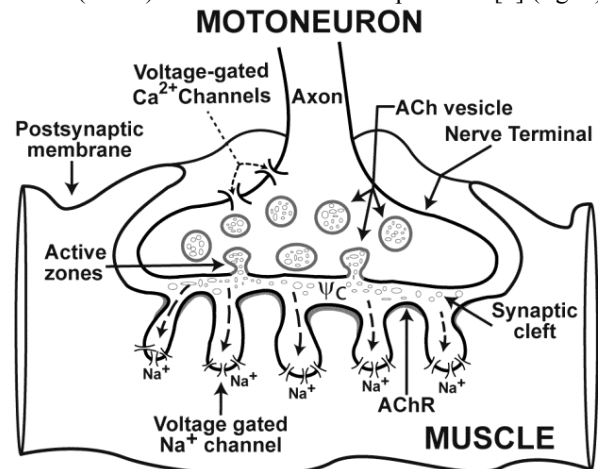


Fig. 1. Schematic diagram of the NMJ transmission process.

The flow of ions through the weakly opened sodium channels generates a current along the synaptic cleft (15–200 nm, [8]) which affects the local extracellular potential at the junction, and through a positive feedback boosts channels activation [9]. In this paper, we present a novel and realistic NMJ model to study the effect of sodium channels contribution in generation of the extracellular potential at the cleft and the properties of the synapse itself.

## II. THE MODEL AND ITS PARAMETERS

A frog NMJ was designed using a 50  $\mu\text{m}$  diameter, 500  $\mu\text{m}$  long barrel shaped muscle fiber and a circular axon terminal of 19.5  $\mu\text{m}$  radius ( $r_a$ ) with real physiological parameters to simulate the transmission process (equivalent electrical circuit in fig. 2) [8]. The muscle membrane with  $7.85 \times 10^{-8} \text{ m}^2$  surface area was separated by a cleft distance of 50 nm ( $d_c$ ) [8]. To mimic the synaptic transmission and generate action potentials at the muscle fiber incorporating the current flow in

Manuscript received March 29, 2012.

Mufti Mahmud is with the NeuroChip Laboratory of Department of Biomedical Sciences, University of Padova, 35131, Padova, Italy and Institute of Information Technology, Jahangirnagar University, Savar, 1342 – Dhaka, Bangladesh (Corresponding Author; phone: +39 049 8275308; fax: +39 049 8275331; e-mail: mahmud@dei.unipd.it)

M. Mostafizur Rahman is with the NeuroChip Laboratory of Department of Biomedical Sciences and Department of Information Engineering, University of Padova, 35131, Padova, Italy (e-mail: rahman@dei.unipd.it)

Stefano Vassanelli is with the NeuroChip Laboratory of Department of Biomedical Sciences, University of Padova, 35131, Padova, Italy (e-mail: stefano.vassanelli@unipd.it)

the cleft, we first studied the behavior of the sodium channels at the NMJ. In this way, first the maximum sodium conductance at the muscle infold,  $\bar{g}_f^{Na}$  (eq. 3) was calculated using the sodium channel conductance  $2.75 \times 10^{-13}$  S/channel ( $g_f^{Na}$ ) [10] and sodium channel density  $80 \times 10^{10}$  channels/m<sup>2</sup> ( $\rho_f^{Na}$ ) of the infold [11] to determine sodium conductance at the end plate, in turn calculate the sodium conductance of the synaptic area  $G_s$  (eq. 1). The sodium channel activation at muscle endplate ( $g_e^{Na}$ ) (eq. 2) was calculated using the standard Hodgkin-Huxley formalism (HHF) where  $m_e$  and  $h_e$  are the channel activation and inactivation probability [12].

$$G_s = \pi g_e^{Na} \cdot r_a^2 \quad (1)$$

Where,

$$g_e^{Na} = \bar{g}_f^{Na} m_e^3 h_e \quad (2)$$

$$\bar{g}_f^{Na} = g_f^{Na} \rho_f^{Na} \quad (3)$$

The global resistance at the cleft,  $\delta_c$  (eq. 4) was derived using cable equation and point contact model [9, 13-16].

$$\delta_c = \frac{\delta_s}{\pi \epsilon_s^2} \left( \frac{\epsilon_s l_0(\epsilon_s)}{2l_1(\epsilon_s)} - 1 \right) \quad (4)$$

With, sheet resistance  $\delta_s$  (eq. 5) and sheet constant  $\epsilon_s$  (eq. 6)

$$\delta_s = \frac{\delta_j}{d_c} \quad (5)$$

where electrolyte resistance  $\delta_j$  is 0.1 K $\Omega$  cm

$$\epsilon_s = r_a \sqrt{\delta_s g_e^{Na}} \quad (6)$$

The  $l_0$  and  $l_1$  are the modified Bessel functions.

The junction potential ( $\psi_c$ ) was calculated iteratively using the eq. 7 with membrane potential  $\psi_m$  computed using standard HHF [12] and sodium reversal potential  $\psi_0$ .

$$\psi_{c+1} = (\psi_m - \psi_c - \psi_0) \frac{G_s \delta_c}{1 + G_s \delta_c} \quad (7)$$

Now the endplate sodium current ( $J_e^{Na}$ ) (eq. 8) was computed using the previously calculated entities ( $G_s$ ,  $\psi_m$ ,  $\psi_c$ ) and sodium Nernst equilibrium potential  $\psi_{Na}$ .

$$J_e^{Na} = G_s \cdot (\psi_m - \psi_c - \psi_{Na}) \quad (8)$$

Similarly, the AChR current at the endplate ( $J_e^{AChR}$ ) was computed through calculation of maximum AChR conductance at the endplate ( $\bar{g}_e^{AChR}$ ) using AChR density  $1.86 \times 10^{-13}$  S/channel [10] and AChR conductance  $10 \times 10^{11}$  channels/m<sup>2</sup> [11] at the muscle membrane (eq. 9). Also, the contribution of AChR activation probability  $P^{AChR}$ ,  $\psi_m$ , and synaptic impact using a double exponential function with activation decay time ( $\tau_d$ )  $1.43 \times 10^{-3}$  s and raise time ( $\tau_r$ )  $0.6 \times 10^{-3}$  s [17] was taken into consideration.

$$J_e^{AChR} = \bar{g}_e^{AChR} P^{AChR} \psi_m \left( \frac{1}{e^{\tau - \tau_d}} - \frac{1}{e^{\tau - \tau_r}} \right) \quad (9)$$

Eventually, the final stimulus current  $J_e^{stim}$  (eq. 10) was the combined contribution of  $J_e^{AChR}$  and  $J_e^{Na}$  to compute the muscle membrane potential,  $\psi_m$  (eq. 11) [18-20].

$$J_e^{stim} = J_e^{AChR} + J_e^{Na} \quad (10)$$

$$\psi_m C_m = -(J_m^{Na} + J_m^K + J_m^L + J_e^{stim}) \quad (11)$$

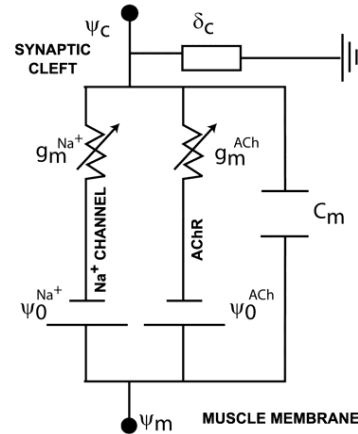


Fig. 2. Equivalent electrical circuit of the NMJ.

### III. SIMULATED RESULTS AND DISCUSSIONS

Voltage-clamp experiments were simulated in MATLAB through scripting (version: R2009b; www.mathworks.com).

To study the sodium channels effect on generation of potentials at the junction and in the postsynaptic muscle membrane, we simulated junction potentials and membrane potentials using the aforementioned model.

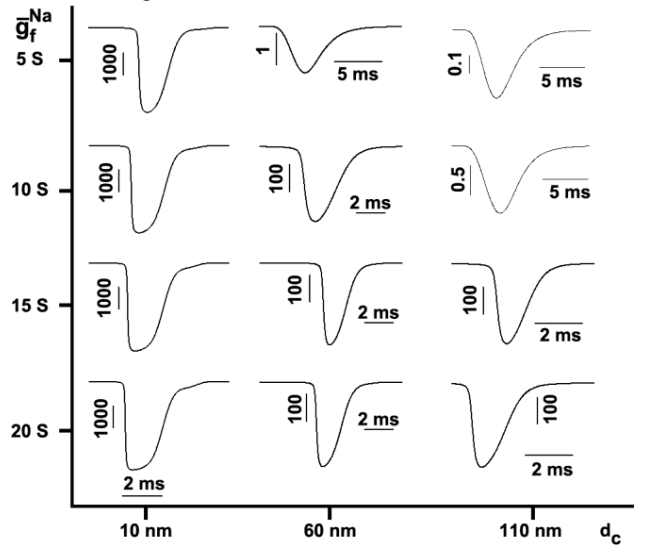


Fig. 3. Global resistances of the synaptic cleft at different maximum sodium conductance and cleft distance. Values are in K $\Omega$ . The resistance starts from a maximum value and goes down as sodium channels permeability increases.

We varied the amount of activated voltage-gated sodium channels at the muscle infolds (obtained by calculating the maximum global conductance of sodium channels at the muscle infolds and varied from 5 S to 20 S) and the cleft distance (10, 60, and 110 nm), and noted the parameters which play important role in synaptic transmission (e.g., global resistance of the cleft). As shown in fig. 3, the  $\delta_c$  depends on both the amount of activated sodium channels as

well as the cleft distance. The increasing cleft distance increases the resistance as well, thus, reducing the signal transduction capability. However, the effect of reduced signal is compensated by increasing the number of activated sodium channels due to the positive feedback provided by the endplate sodium current at the junction ( $J_e^{Na}$ ).

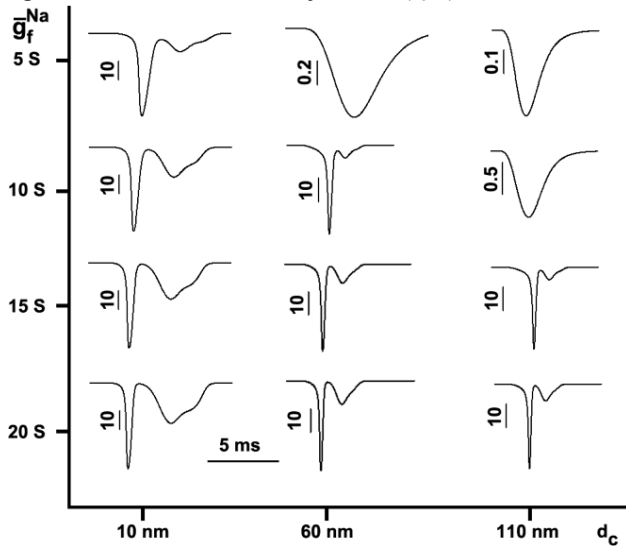


Fig. 4. Extracellular junction potential at the synaptic cleft for different global resistances of the synaptic cleft calculated for varied amount of sodium channel action and synaptic cleft height. Values are in mV.

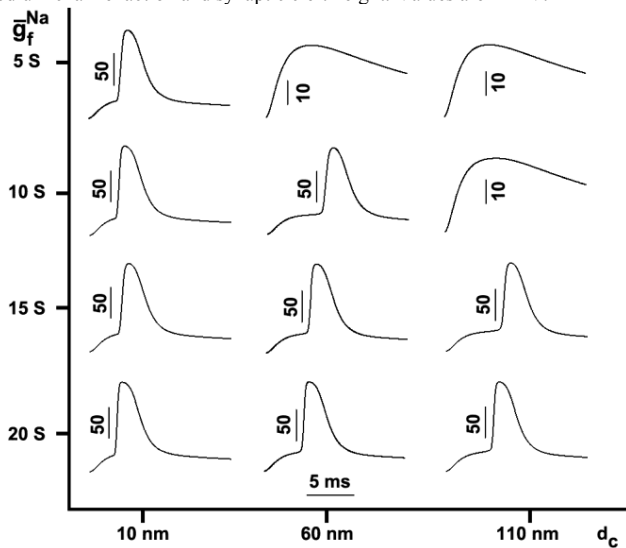


Fig. 5. Postsynaptic muscle membrane potentials resulting from combined effects of variation of  $\delta_c$ , increase in infold sodium channels permeability, and  $\psi_c$ . Values are in mV.

The effect of changes in the global resistance of the cleft is also reflected in the extracellular potentials at the junction ( $\psi_c$ ) (fig. 4). Though the initial cause of the  $\psi_c$  generation at the cleft is the weakly opened sodium channels, yet, this gets amplified due to reduced  $\delta_c$  (caused by narrow cleft distance)

and increased sodium channels permeability (caused by high maximum sodium channel conductance). As the global sodium conductance of the synaptic area is proportional to the endplate sodium permeability, this increase in permeability in turn increases the global conductance and generates higher amount of junction potential which initially is considered to be zero.

Again, increase in the infold sodium channel permeability due to the high maximum sodium channels conductance opens up more sodium channels in the muscle infolds causing sharp depolarization of the postsynaptic muscle membrane which initiates the action potentials from a resting potential of  $-95$  mV (fig. 5).

This effect of sodium channels is almost negligible when a wide synaptic cleft is considered with a limited amount of activated sodium channels in the junction. As a result, we could see that the global resistance of the cleft remains very high, generates small junction potential, and fails to initiate action potentials in the postsynaptic muscle membrane (in figs. 3, 4, and 5: (5 S, 60 nm), (5 S, 110 nm), (10 S, 110 nm)).

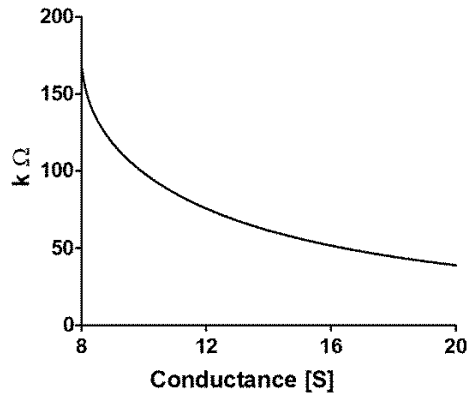


Fig. 6. Profile of the global resistance of the synaptic cleft ( $\delta_c$ ) for different maximum conductances of the sodium channels ( $d_c=50$  nm).

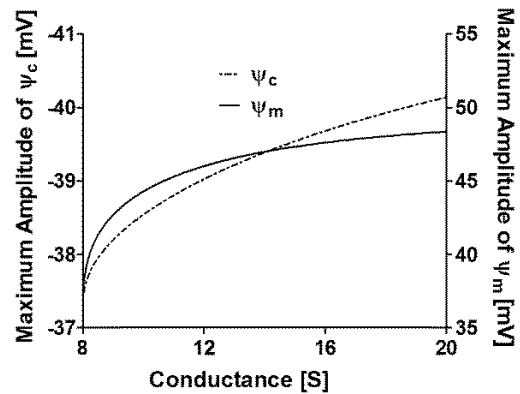


Fig. 7. Profiles of extracellular junction potential ( $\psi_c$ ) in the left y-axis and membrane potential ( $\psi_m$ ) in the right y-axis calculated for different sodium channels maximum conductance ( $d_c=50$  nm).

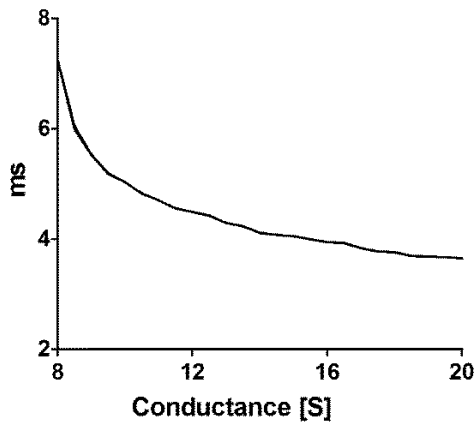


Fig. 8. Profile of onset latency of postsynaptic membrane potential ( $\psi_m$ ) for different maximum sodium conductance values ( $d_c=50$  nm).

Fig. 6 further illustrates the effect of the amount of sodium channel activation on the global resistance of the synaptic cleft. The profile was computed by calculating the minimum values of the resistance curves resulting from applying different maximum sodium channels conductances from 8 to 20 S with a step of 0.1 S. We can see the resistance gradually reduces with the increasing activation of the channels.

Fig. 7, on the other hand, shows the effect of maximum sodium channel conductance on amplitude of the extracellular potential at the junction (left y-axis) and on amplitude of the action potential triggered at the postsynaptic muscle membrane (right y-axis). Amplitudes of both the entities increase with the increasing amount of sodium channel activation. The amplitude increase of the action potential is a direct consequence of the positive feedback provided by the junction potential in boosting the sodium channel activation.

Fig. 8 shows the latency of the action potential onset which decreases with increasing maximum sodium channels conductances. This denotes that the efficiency of the synaptic transmission at the neuromuscular junction in terms of action potential generation and propagation largely depends on the amount of activated sodium channels at the muscle infolds.

Efficient synaptic transmission demonstrated by our model is due to the flow of current at the synaptic cleft which modifies the local extracellular potential at the junction and in the adjacent membranes' voltage-dependent processes as previously demonstrated at a cell-to-substrate adhesion [9].

#### IV. CONCLUSION

The NMJ plays an important part in our motor movement. To understand the NMJ transmission process and to better represent the biological mechanisms a realistic model is required to address therapeutic solutions for motor disorders caused by dysfunction of the NMJ. In this work, we first

presented a realistic NMJ model taking into account the flow of current at the extracellular space and performed simulations to study the effect of activated sodium channels quantity and cleft height on the synaptic transmission process. Through cleft's global resistance, extracellular junction potential and postsynaptic membrane potential we showed that the sodium channels at the postsynaptic muscle membrane infolds alter the synaptic transmission process.

#### REFERENCES

- [1] W. Hoch, "Formation of the neuromuscular junction," *Eur. J. Biochem.*, Vol. 265, pp. 1-10, 1999.
- [2] J.R. Sanes, J. W. Lichtman, "Development of the Vertebrate Neuromuscular Junction," *Annu Rev Neurosci*, Vol. 22, pp. 389-442, 1999.
- [3] G. Davis, C. Goodman, "Genetic analysis of synaptic development and plasticity: homeostatic regulation of synaptic efficacy," *Curr. Opin. Neurobiol.*, Vol. 8, pp. 149-156, 1998.
- [4] M. Thomas, G. Bruce, "Formation of the neuromuscular junction: molecules and mechanisms," *Bioessays*, Vol. 20, pp. 819-829, 1998.
- [5] M.R. Deschenes, C.M. Maresh, W.J. Kraemer, "The neuromuscular junction structure, function, and its role in the excitation of muscle," *J. Strength Cond. Res.*, Vol. 8, pp. 103-109, 1994.
- [6] W. Zach, R. Joshua, "Synaptic structure and development: the neuromuscular junction," *Cell*, Vol. 72, pp. 99-121, 1993.
- [7] A. Martin, "Amplification of neuromuscular transmission by postjunctional folds," *Proc. R. Soc. B*, Vol. 258, pp. 321-326, 1994.
- [8] S.J. Wood, C.R. Slater, "Safety Factor at the Neuromuscular Junction," *Prog. Neurobiol.*, Vol. 64, No. 4, pp. 393-429, 2001.
- [9] P. Fromherz, "Self-Gating of Ion Channels in Cell Adhesion," *Phys. Rev. Lett.*, Vol. 78, No. 21, pp. 4131-4134, 1997.
- [10] C.A. Lewis, "Ion-Concentration Dependence of the Reversal Potential and the Single Channel Conductance of Ion Channels at the Frog Neuromuscular Junction," *J Physiol.*, Vol. 286, pp. 417-445, 1979.
- [11] J.H. Caldwell, D.T. Campbell, K.G. Beam, "Na Channel Distribution in Vertebrate Skeletal Muscle," *J Gen. Physiol.*, vol. 87, pp. 907-932, 1986.
- [12] A.L. Hodgkin, A.F. Huxley, "A quantitative description of membrane current and its application to conduction and excitation in nerve," *J. Physiol.*, Vol. 117, pp. 500-544, 1952.
- [13] P. Fromherz, C.O. Muller, R. Weis, "Neuron-transistor: electrical transfer function measured by the patch-clamp technique," *Phys Rev Lett*, Vol. 71, pp. 4079-4082, 1993.
- [14] R. Weis, P. Fromherz, "Frequency dependent signal-transfer in neuron-transistors," *Phys Rev E*, Vol. 55, pp. 877-889, 1997.
- [15] R. Schatzthauer, P. Fromherz, "Neuron-silicon junction with voltage-gated ionic currents," *Eur J Neurosci*, Vol. 10, pp. 1956-1962, 1998.
- [16] S. Vassanelli, P. Fromherz, "Transistor-records of excitable neurons from rat brain," *Appl Phys A*, Vol. 66, pp. 459-463, 1998.
- [17] S.D. Head, "Temperature and endplate currents in rat diaphragm," *J. Physiol.*, Vol. 334, pp. 441-459, 1983.
- [18] M.M. Rahman, M. Mahmud, S. Vassanelli, "Self-Gating of sodium channels at neuromuscular junction," In: *Proc. 5th IEEE EMBC Conf. Neural Eng. (NER2011)*, Cancun, Mexico, 2011, pp. 208-211.
- [19] M.M. Rahman, M. Mahmud, S. Vassanelli, "Sodium channels' kinetics under self-gating condition at neuromuscular junction," In: *2011 Proc. 4th Intl. Conf. Biomed. Eng. Inf. (BMEI2011)*, Shanghai, China, 2011, pp. 990-994.
- [20] M.M. Rahman, M. Mahmud, S. Vassanelli, "Effect of Self-Gating on Action Potential Firing at Neuromuscular Junction," In: *Conf. Proc. IEEE Eng. Med. Biol. Soc.*, Boston, USA, 2011, pp. 4082-4085.